PHYSICAL REVIEW A VOLUME 49, NUMBER 5 MAY 1994

Electron-pair wave packets

Lijun Zhang and James M. Feagin
Department of Physics, California State University-Fullerton, Fullerton, California 92634

Volker Engel
Fakultät für Physik, Universität Freiburg, 79104 Freiburg, Germany

Aiichiro Nakano
Concurrent Computing Laboratory for Material Simulation, Department of Physics and Astronomy, Louisiana State University, Baton Rouge, Louisiana 70803-4001

(Received 15 September 1993)

We present a computational scheme to propagate wave packets describing S states of two-electron systems. Body-fixed polar coordinates (r_1, r_2, θ) are used to represent the time-dependent wave functions on a grid in three dimensions. We handle the Coulomb singularities by transformation of the wave function and a modified finite-difference formula to evaluate the kinetic energy. We use a finite-difference split-operator scheme for the time propagation and, as a first application, we compute the low-energy spectrum of helium and H^-.

PACS number(s): 31.15.+q, 31.70.Hq, 34.50.Fa

I. INTRODUCTION

The three-body Coulomb problem characterized by helium and H^- continue to take a central role in atomic and molecular physics. Despite enormous effort in quantum mechanics since its inception, and in classical mechanics with the analogous three-planet problem since early in the past century, a comprehensive description remains unknown. Nevertheless, considerable progress has been made on several fronts, theoretically and especially experimentally [1,2].

The problem naturally separates into two regimes distinguished by total energy either above or below the threshold for three-body breakup [3]. Below threshold, the concern is with resonance states which dissociate into electron-atom or electron-ion channels, while above threshold, the issue is the correlated three-particle motion generated by excitation from below threshold. Of particular interest is the connection of high-lying electron-pair levels below threshold with Wannier ridge states above, specifically, the link between bound and continuum states of the electron pair. Just above threshold, basic features of these states can be described analytically, albeit approximately, by the Wannier theory [4–7]. Just below threshold little is known, although a great deal has been speculated on the association of the density and widths of electron-pair resonances with the (Wannier) threshold double-ionization law [8]. Further below threshold, very accurate basis-set results now exist [9–13] for the positions and widths of singly and doubly excited resonances and a great deal of progress has been made in categorizing their properties by invoking a classical point of view [14] as well as an analogy with simple molecules [15].

Many details of a dynamical process can be revealed by examining the time propagation of wave packets. The advantage of the idea is its ease of implementation. The main disadvantage is the restriction to processes with few dimensions imposed by present-day computer-storage limitations and ultimately computer speed. If the past five years are any indication, however, the situation is likely to improve dramatically in the next few years [16]. Along with the recent advances in hardware, great progress has been made in finding efficient techniques for solving the time-dependent Schrödinger equation directly. These methods have proven to be stable and accurate [17] and to eliminate the need for perturbation theory with respect to particle-particle and particle-field interactions. The power of these methods has been noticed by a broad community whose interests include molecular quantum dynamics [18], femtosecond spectroscopy [19], strong-field atomic ionization [20], ion-atom [21], ion-nucleus [22] and atom-surface [23] collision, as well as quantum well spectroscopy [24]. A thorough introduction to this area of theoretical physics is provided by a special issue of *Computer Physics Communications* [25] devoted entirely to the subject of time-dependent methods for quantum dynamics.

The goal of this paper is to develop a lattice method capable of studying the motion of electron-pair wave packets near the double-ionization threshold. The basic notion is to achieve a direct, even if approximate, description of both bound and continuum electron-pair states, which avoids reliance on basis sets but nevertheless faithfully describes Coulomb long-range effects and singularities. Ideally, we would set up this six-dimensional problem on a six-dimensional lattice using three Cartesian coordinates for each electron (with the nucleus fixed as the system center of mass). This would allow a relatively direct computation because the Coulomb singularities could be handled simply by arranging them between lattice points. At present, howev-

1050-2947/94/49(5)/3457(6)/$06.00 © 1994 The American Physical Society

er, computer memory constrains us to smaller lattices and fewer dimensions. Hence, we consider only $L=0$ total angular momentum of the electron pair, i.e., S states, in order to reduce the problem to three dimensions. This requires the introduction of polar coordinates, for example, r_1 and r_2 of the two electrons with respect to the nucleus and θ the interelectronic angle. Polar coordinates and the representation of Coulomb singularities, however, introduce additional numerical difficulties, and this paper is also about settling these issues.

We propagate wave packets directly in real and imaginary time by taking a succession of small time steps, but otherwise evaluating the full time-development operator on a lattice. With a specified lattice, we improve upon analogous quantum Monte Carlo methods [26], which are limited essentially to determining ground states. Although the present approach is rather similar to methods involving fast Fourier transforms [27,28], we conduct a finite-difference approximation of the kinetic energy [29,30] and perform all computations in coordinate space. As a first step, we compute in this paper the low-energy spectrum of helium and H^- and demonstrate the essential features of the method. Our ongoing work will involve wave packets along the Wannier ridge.

II. THEORY

We seek solutions of the time-dependent Schrödinger equation for a three-body Coulomb system defined by one nucleus, charge Z, and two electrons. Assuming the nucleus to be the center of mass of the system, the Hamiltonian can be written as

$$H=-\tfrac{1}{2}\nabla_1^2-\tfrac{1}{2}\nabla_2^2-\frac{Z}{r_1}-\frac{Z}{r_2}+\frac{1}{r_{12}} \ . \tag{1}$$

We use atomic units throughout this paper. For total angular momentum $\mathbf{L}_T=\mathbf{L}_1+\mathbf{L}_2=0$, the six-dimensional problem reduces to three dimensions. In what follows we use body-fixed coordinates r_1, r_2, and θ, where the radial coordinates r_i denote electron-nucleus separation and θ is the angle between the vectors $\mathbf{r}_1$ and $\mathbf{r}_2$. The Hamiltonian then takes the form

$$H=-\tfrac{1}{2}\frac{1}{r_1^2}\frac{\partial}{\partial r_1}r_1^2\frac{\partial}{\partial r_1}-\tfrac{1}{2}\frac{1}{r_2^2}\frac{\partial}{\partial r_2}r_2^2\frac{\partial}{\partial r_2}+b(r_1,r_2)L^2+V(r_1,r_2,\theta) \ . \tag{2}$$

Here the angular-momentum operator squared L^2 and its coefficient $b(r_1,r_2)$ are defined by

$$L^2=-\frac{1}{\sin\theta}\frac{\partial}{\partial\theta}\sin\theta\frac{\partial}{\partial\theta}, \quad b(r_1,r_2)=\tfrac{1}{2}\left[\frac{1}{r_1^2}+\frac{1}{r_2^2}\right] , \tag{3}$$

and

$$V(r_1,r_2,\theta)=-\frac{Z}{r_1}-\frac{Z}{r_2}+\frac{1}{\sqrt{r_1^2+r_2^2-2r_1r_2\cos\theta}} \tag{4}$$

is the potential energy. The Hamiltonian (2) exhibits singularities at $r_1=r_2=0$ and at $\theta=0$ and π. As we will describe in detail below, we evaluate the derivatives by finite differencing. It is therefore convenient to force the wave function to be zero at these singular points [31]. This can be done by transforming the original wave function $\varphi(r_1,r_2,\theta)$ according to

$$\psi=r_1r_2\sqrt{\sin\theta}\,\varphi \ . \tag{5}$$

The Hamiltonian acting on the "reduced" wave function $\psi(r_1,r_2,\theta)$ is then

$$H=T_{r_1}+T_{r_2}+b(r_1,r_2)l^2+V(r_1,r_2,\theta) , \tag{6}$$

where $T_{r_i}=-\frac{1}{2}\partial^2/\partial r_i^2$ denotes the kinetic-energy operator of electron (i) and

$$l^2=-\frac{\partial^2}{\partial\theta^2}-\frac{1}{4}\frac{1}{\sin^2\theta}-\frac{1}{4} \tag{7}$$

is the transformed angular-momentum operator.

For the time development, we use a short-time propagator that can be approximated as

$$U(\lambda)=e^{\lambda V/2}e^{\lambda T_{r_1}/2}e^{\lambda T_{r_2}/2}e^{\lambda b l^2}e^{\lambda T_{r_1}/2}\times e^{\lambda T_{r_2}/2}e^{\lambda V/2}+O(\lambda^3) , \tag{8}$$

where $\lambda=-i\,dt$ with dt the time-propagation step size. The wave function at time $T=n\,dt$ is thus obtained by successive application of the short-time propagator on the initial function. The symmetrical splitting (8) ensures that the error is of order λ^3 [29,31,32]. The computational details of the time propagation will be discussed in Sec. III.

Information about the system's eigenstates can be obtained from the time-correlation function

$$c(t)=\langle\psi(0)|\psi(t)\rangle , \tag{9}$$

which measures the overlap between an initial $t=0$ wave packet and the time-developed state at time t. Correlation functions of the form (9) are frequently used for the interpretation of molecular spectra [33–35]. However, it is computationally more effective to evaluate the function

$$d(t)=\langle\psi(-t)|\psi(t)\rangle=c(2t) \ . \tag{10}$$

The relation of $d(t)$ to the correlation function $c(2t)$ shows that $c(T)$ can be obtained from propagation of the wave packet just up to $T/2$ [36].

The system energy spectrum can be extracted by a Fourier transform of the time-correlation function, i.e.,

$$\sigma(E)\sim\int_{-\infty}^{+\infty}dt\,e^{iEt}c(t) \ . \tag{11}$$

Since $c(-t)=c^*(t)$, the spectrum $\sigma(E)$ is a real number which is, in fact, closely related to the "Fermi's golden rule" expression for dipole transition rates [35].

Another way to extract information about the eigenstates of a system is to propagate an initial wave packet in imaginary time, i.e., by setting $\lambda=-dt$ in Eq. (8). It is readily seen that for long enough propagation times the wave packet "relaxes" or "diffuses" to the ground state since all excited-state components of the propagated wave packet decay to zero. This technique is commonly used in quantum Monte-Carlo (QMC) calculations of eigenenergies in many-body systems [37], but has the capability over QMC of calculating excited states [38].

III. TIME PROPAGATION

A. Radial propagation

For the time propagation we require the kinetic-energy operator acting on an arbitrary wave function. We evaluate the second derivatives by finite differencing; for details see Refs. [26,27]. Consider, for example, a kinetic-energy operator T_r acting on the wave function $\psi(r_n)=\psi_n$ defined by a spatial grid with points r_n such that $r_{n+1}-r_n=\Delta r$. In second order one obtains

$$(T_r\psi)_n=\frac{1}{2(\Delta r)^2}\{-\psi_{n-1}+2\psi_n-\psi_{n+1}\} . \tag{12}$$

Since the above formula connects the wave function at r_n symmetrically to the function at the nearest-neighbor points, the matrix representation of T_r consists of a tridiagonal, symmetric matrix. In our case the wave function $\psi(r_1,r_2,\theta)$ vanishes at the ends of the grids [see Eq. (5)], although the wave packet does not have to be periodic.

For the time propagation, we write the tridiagonal matrix as a direct sum of two block-diagonal matrices T_r^E and T_r^O and split the short-time propagator symmetrically:

$$e^{\lambda T_r}=e^{\lambda T_r^E/2}e^{\lambda T_r^O}e^{\lambda T_r^E/2} . \tag{13}$$

This expression is exact through second order, consistent with the splitting in Eq. (8). Since the blocks appearing in the matrices $T_r^{E,O}$ are symmetrical 2×2 matrices, the exponentiation can be performed analytically.

One thus obtains

$$\begin{aligned}(e^{\lambda T_r^E/2}\psi)_n=&+\frac{1-(-1)^n}{2}\beta_E\psi_{n-1}+\alpha_E\psi_n\\&+\frac{1+(-1)^n}{2}\beta_E\psi_{n+1}\end{aligned} \tag{14}$$

and

$$\begin{aligned}(e^{\lambda T_r^O}\psi)_n=&+\frac{1+(-1)^n}{2}\beta_O\psi_{n-1}+\alpha_O\psi_n\\&+\frac{1-(-1)^n}{2}\beta_O\psi_{n+1} ,\end{aligned} \tag{15}$$

where at the grid boundaries $(e^{\lambda T_r^O}\psi)_0=\exp\{\lambda/[2(\Delta r)^2]\}\psi_0$, $(e^{\lambda T_r^O}\psi)_{N-1}=\exp\{\lambda/[2(\Delta r)^2]\}\psi_{N-1}$, and also

$$\begin{aligned}\alpha_E&=\tfrac{1}{2}\{1+e^{\lambda/[2(\Delta r)^2]}\} ,\\ \beta_E&=\tfrac{1}{2}\{1-e^{\lambda/[2(\Delta r)^2]}\} ,\end{aligned} \tag{16}$$

and

$$\begin{aligned}\alpha_O&=\tfrac{1}{2}\{1+e^{\lambda/(\Delta r)^2}\} ,\\ \beta_O&=\tfrac{1}{2}\{1-e^{\lambda/(\Delta r)^2}\} .\end{aligned} \tag{17}$$

The evaluation of the kinetic part of the short-time propagator with the finite-difference formula as expressed by the above equations will be called the "finite-difference–split-operator" (FD–SPO) technique in what follows. The name is lent from the "Fourier transform–split-operator" technique (FT–SPO) [29]. The latter splits the kinetic and the potential part of the propagator, and the kinetic energy is evaluated by fast Fourier transforms. In our case, the kinetic and the potential energy part of the propagator are also split [see (8)], but an additional splitting of the kinetic energy (13) is necessary as well.

It is of interest to compare the efficiency of the FD–SPO and FT–SPO schemes. A Fourier transform in one dimension requires $N\log_2N$ operations, where N is the number of grid points. At each time step, one needs two transforms, into and out of the momentum representation. The FD–SPO scheme requires only N operations for the second derivatives, but $3N$ operations to evaluate the three exponential operators in Eq. (13). In principle, therefore, the finite-difference scheme requires less computational effort as the number of grid points increases. There is, however, another consideration. The FD–SPO error in the time propagation (13) scales as $\lambda/(\Delta r)^2$ since $T_r\sim1/(\Delta r)^2$. This means that in order to achieve the same accuracy with double the number of points, the time step has to be reduced by a factor of 4. With Fourier transforms, on the other hand, time-step size and grid parameters are mostly independent (see the discussion regarding Fig. 1).

B. Angular propagation

In the preceding section, we transformed the angular-momentum operator Eq. (3) and obtained Eq. (7) in order to implement the split-operator approximation in the time development. In short, the split of the time-development operator requires stand-alone derivatives with coefficients independent of derivative coordinates. With the transformed angular-momentum operator (7) we can then directly introduce a finite-difference approximation for the second derivative with respect to θ.

One readily finds, however, that the conventional finite-difference formula Eq. (12) applied as a function of θ to the transformed wave function ψ develops severe inaccuracies near the grid boundaries $\theta=0$ and π. The difficulty arises because the second derivative becomes infinite near the boundaries since $\psi\sim\sqrt{\sin\theta}$ there, so that l^2 in Eq. (7) becomes difficult to approximate with just three values of ψ. Instead, we note that

$$l^2\sqrt{\sin\theta}=0 \tag{18}$$

is an identity that holds for all θ. Therefore, we introduce a modified finite-difference approximation for l^2 directly according to

$$(l^2\psi)_k\equiv-\frac{1}{(\Delta\theta)^2}\{\psi_{k-1}-2a_k\psi_k+\psi_{k-1}\} , \tag{19}$$

where a_k is a correction which we defined by requiring that Eq. (19) holds. Thus, substituting $\psi_k=\sqrt{\sin(k\Delta\theta)}$ into (19) and enforcing (18), we have

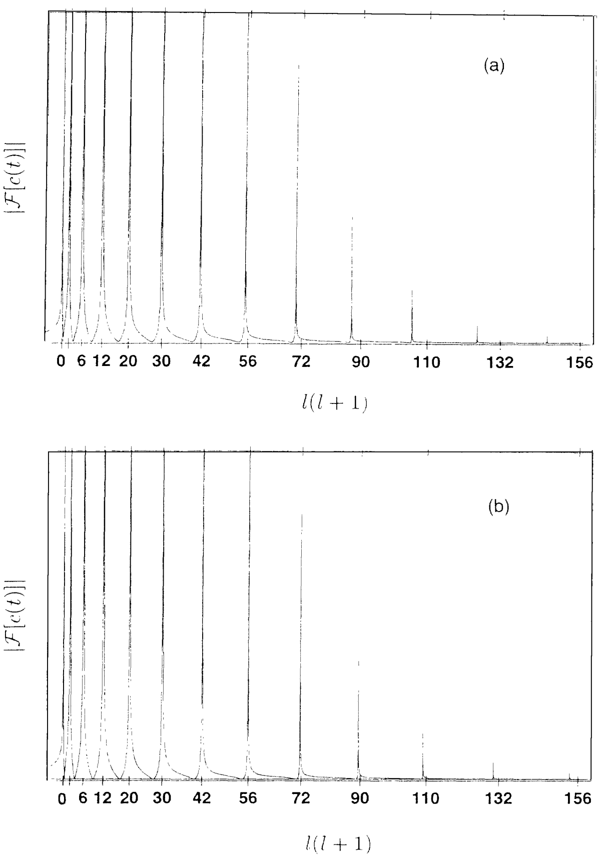

FIG. 1. Angular-momentum spectrum: (a) Number of grid points $N=40$ and $\Delta\theta=\pi/41$; (b) number of grid points $N=70$ and $\Delta\theta=\pi/71$.

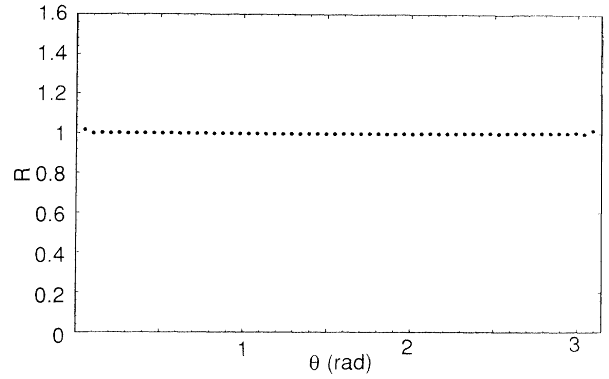

FIG. 2. The plot of $R(\theta)$ vs θ where $R(\theta)=\psi(\theta,t_{\max})/\psi(\theta)_{gd}$ where $\psi(\theta)_{gd}=(1/\sqrt{2})\sqrt{\sin\theta}$ and $t_{\max}=10$; the exact value is $R=1$.

$$a_k=\frac{1}{2}\frac{\sqrt{\sin[(k+1)\Delta\theta]}+\sqrt{\sin[(k-1)\Delta\theta]}}{\sqrt{\sin(k\Delta\theta)}} . \tag{20}$$

Near the middle of the lattice the wave function ψ and its derivatives are finite, and we expect our approximation (19) to reduce to the conventional finite-difference formula Eq. (12) with $a_k=1$. Setting $k=\frac{1}{2}N$ in (20) and noting that $\frac{1}{2}N\Delta\theta=\frac{1}{2}\pi$, we see that $a_{N/2}\sim 1$, as desired.

We tested Eq. (19) by computing the time evolution of a Gaussian wave packet given by

$$\psi(0)=\sqrt{\sin\theta}\, e^{-(\pi-\theta)^2} . \tag{21}$$

The angular-momentum spectrum was calculated from the Fourier transform of the time-correlation function (9) which was computed up to a time $t_{\max}=65.5$. Figure 1(a) shows that with $N=40$ grid points the spectrum is fairly well represented up to about $L=5$. Figure 1(b) shows that with $N=70$ grid points convergence improves up to about $L=8$.

Finally, we performed the same propagation in complex time. As one readily shows, $\psi(t\rightarrow\infty)$ converges to the $l=0$ ground state of l^2, namely, $\sqrt{\sin\theta}$. Thus, in Fig. 2, we plot the ratio $l^2\psi(\theta,t_{\max})/\sqrt{\sin\theta}$ as a function of θ, where the maximum propagation time was $t_{\max}=10$. The closeness of the ratio to unity across the grid, except very near the ends of the grid, reinforces our confidence in the approximation (19).

IV. APPLICATION TO HELIUM AND H$^-$

As a first application of the computational method outlined in the preceding section, we propagated a two-electron helium wave packet in imaginary time $\lambda=-dt$. We took as initial function

$$\psi(0)=r_1 r_2\sqrt{\sin\theta}\, e^{-r_1^2-r_2^2} e^{-(\pi-\theta)^2} , \tag{22}$$

and used 60 grid points for each of the radial coordinates in the range $0<r_i<6$ and 28 points for the angular coordinate in the range $0<\theta<\pi$. We used $dt=3\times 10^{-5}$ for the time-step size. After a total propagation time $t_{\max}=50$, we obtained -2.87 for the ground-state energy and an overall error of $\sim 1\%$ compared to the accepted value $-2.903\,72$ [39].

We then propagated in real time with the same initial function (22). We increased each radial grid, however, to 128 points in the range $0<r_i<20$ but reduced the angular interval to 24 points. The angular-momentum contribution $\exp\{\lambda b(r_1,r_2)l^2\}$ requires the smallest time step during the propagation. This stems from the fact that it contains a factor of $\lambda/\{(\Delta\theta)^2(\Delta r)^2\}$ in the exponent. The time-development algorithm is therefore optimized by using a separate, smaller time step for the angular-momentum contribution [40].

We note in passing that the algorithm we use is ideal for parallel computing because the operations in Eqs. (14) and (15) require communication only between nearest-neighbor elements on the lattice.

Figure 3 shows the calculated spectrum for helium. It reveals a large peak at -2.87 followed by an energy gap of ~ 0.5. The peak clearly belongs to the ground state. The next higher peak appears at -2.146, just where the exact spectrum begins to show structure above the ground state [10,39]. Although we do not resolve the excited states, we consider these results satisfactory because of the accurate representation of the ground state and the energy gap above. The energy resolution of ~ 0.05 is fixed by the finite propagation time $t_{\max}=131$ used.

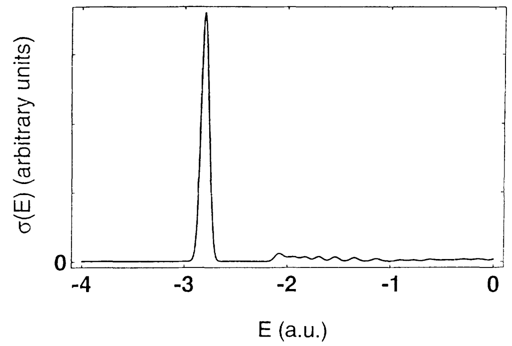

FIG. 3. The low-lying energy spectrum of helium computed from the Fourier transform Eq. (11) of the correlation function Eq. (9).

Also, the spatially extended, excited-state wave functions are not fully represented by the radial grid used here. Note that the large ground-state peak is due to the large component of the ground state in the initial wave packet.

The helium computations described above are easily converted to other two-electron systems. Thus we calculated the ground state and correlation function of H^- simply by changing $Z=2$ to $Z=1$ and doubling the length of each radial grid (holding, however, the number of grid points fixed), in order to represent the increased size of this loosely bound system. With the imaginary-time propagation, we found the ground-state energy to be -0.52, as compared to the accepted value of $-0.527\,75$ [39]. Consistent with this result, the energy spectrum calculated from the correlation function (9) shows a peak at -0.527. Note that H^- has only a single bound state.

V. CONCLUSION

We have developed a method to propagate *S*-state electron-pair wave packets directly on a three-dimensional polar-coordinate grid. The technique proves to be stable with respect to time propagation of the full three-body Coulomb problem. All spatial derivatives have been calculated by finite differencing. The angular propagation requires special care, and we introduce a modified finite-differencing scheme to remove numerical instabilities near the boundaries of the angular grid. Our approach eliminates need for basis sets while accurately representing the Coulomb singularities and therefore should handle in principle wave packets above and below the three-body breakup threshold.

As a first application, we have calculated ground-state energies of helium and H^- with reasonable accuracy. The results demonstrate the method's ease of implementation, even though the low-lying energy spectrums for these systems can be computed more accurately by other numerical techniques. Our interests are in the study of electron-pair wave packets near the Wannier ridge, for which other methods have shown only limited success. We now have a tool that can be applied to a wide variety of problems including strong-field ionization of hydrogen, electron-hydrogen scattering, and even the effects of impurity atoms in quantum dots and wires.

ACKNOWLEDGMENTS

We appreciate collaboration with J. Briggs, Freiburg University, and useful discussions with A. R. P. Rau on all aspects of the few-body Coulomb problem. L.Z. and J.F. acknowledge financial support of the U.S. Department of Energy, Division of Chemical Sciences, Offices of Basic Energy Sciences and Energy Research. V.E. acknowledges financial support of the Deutsche Forschungsgemeinschaft within the Sonderforschungsbereich 276. J.F. and V.E. acknowledge NATO support for travel between California State University–Fullerton and Freiburg University. We appreciate having the opportunity to perform our computations on the 8192-node MasPar supercomputer located in the Concurrent Computing Laboratory for Materials Simulations at Louisiana State University. These facilities were acquired with grants awarded by the Louisiana Board of Regents through the Louisiana-Education Quality-Support Fund.

---

[1] A. R. P. Rau, Science **258**, 1444 (1992); U. Fano and A. R. P. Rau, *Atomic Collisions and Spectra* (Academic, Orlando, 1986).
[2] V. Schmidt, Rep. Prog. Phys. **55**, 1483 (1992).
[3] J. S. Briggs, Nucl. Phys. A **543**, 127 (1992).
[4] G. H. Wannier, Phys. Rev. **90**, 817 (1953).
[5] R. K. Peterkop, J. Phys. B **4**, 513 (1971).
[6] A. R. P. Rau, Phys. Rev. A **4**, 207 (1971).
[7] J. M. Feagin, J. Phys. B **17**, 2433 (1984).
[8] J. Macek and J. M. Feagin, J. Phys. B **18**, 2161 (1985). See also A. Vollweiter, J. M. Rost, and J. S. Briggs, *ibid.* **24**, L155 (1991), and references therein.
[9] L. Zhang and A. R. P. Rau, Phys. Rev. A **46**, 6933 (1992); **48**, 3567 (1993), and references therein.
[10] K. Richter, J. S. Briggs, D. Wintgen, and E. A. Solov'ev, J. Phys. B **25**, 3929 (1992).
[11] Y. K. Ho, Phys. Rev. A **35**, 2035 (1987); **41**, 1492 (1990).
[12] M. Chrysos, Y. Komninos, Th. Mercouris, and C. A. Nicolaides, Phys. Rev. A **42**, 2634 (1990).
[13] G. W. F. Drake, Nucl. Instrum. Method Phys. Rev. Sect. B **31**, 7 (1988); Phys. Rev. Lett. **26**, 2767 (1990).
[14] K. Richter and D. Wintgen, Phys. Rev. Lett. **65**, 1965 (1990).
[15] J. M. Rost and J. S. Briggs, J. Phys. B **24**, 4293 (1991), and references therein.
[16] A. Nakano, P. Vashishta, and R. Kalia, in *High Performance Computing and its Applications in the Physical Sciences*, edited by D. A. Browne *et al.* (World Scientific, Singapore, in press).
[17] C. Leforestier, R. H. Bisseling, C. Cerjan, M. D. Feit, R.

Friesner, A. Guldberg, A. Hammerich, G. Jolicard, W. Karrlein, H.-D. Meyer, N. Lipkin, O. Roncero, and R. Kosloff, J. Comput. Phys. **94**, 59 (1991).
[18] R. Kosloff, J. Phys. Chem. **92**, 2087 (1988).
[19] V. Engel, Comput. Phys. Commun. **63**, 228 (1991).
[20] For a recent collection of review articles on this topic, see the book *Atoms in Strong Laser Fields,* edited by M. Gavrila (Academic, San Diego, 1992).
[21] N. H. Kwong, K. J. Schaudt, and J. D. Garcia, Comput. Phys. Commun. **63**, 171 (1991).
[22] S. E. Koonin, *Computational Physics* (Benjamin-Cummings, Menlo-Park, 1986).
[23] R. C. Mowrey and D. J. Kouri, Chem. Phys. Lett. **119**, 285 (1985); J. Chem. Phys. **84**, 6466 (1986); **86**, 6140 (1987).
[24] R. Bavli and H. Metiu, Phys. Rev. A **47**, 3299 (1993).
[25] Comput. Phys. Commun. **63**, (1991), special issue on time-dependent methods for quantum dynamics.
[26] C. E. Beckmann and J. M. Feagin, Phys. Rev. A **36**, 4531 (1987), and references therein.
[27] J. A. Feit, J. R. Morris, and M. D. Feit, Appl. Phys. **10**, 129 (1976).
[28] D. Kosloff and R. Kosloff, J. Comput. Phys. **52**, 35 (1983).
[29] H. De Raedt, Comput. Phys. Rep. **7**, 1 (1987).
[30] J. L. Richardson, Comput. Phys. Commun. **63**, 84 (1991).
[31] M. R. Hermann and J. A. Fleck, Jr., Phys. Rev. A **38**, 6000 (1988).
[32] H. Yoshida, Phys. Lett. A **150**, 262 (1990).
[33] R. G. Gordon, Adv. Magn. Reson. **3**, 1 (1978).
[34] E. J. Heller, Acc. Chem. Res. **14**, 368 (1981); E. J. Heller, in *Potential Energy Surfaces and Dynamics Calculations,* edited by D. G. Truhlar (Plenum, New York, 1981).
[35] R. Schinke, *Photodissociation Dynamics* (Cambridge University Press, Cambridge, England, 1992).
[36] V. Engel, Chem. Phys. Lett. **189**, 76 (1992).
[37] M. H. Kalos and P. A. Whitlock, *Monte Carlo Methods* (Wiley, New York, 1986), Vol. 1.
[38] R. Kosloff and H. Tal-Ezer, Chem. Phys. Lett. **127**, 223 (1986).
[39] C. L. Pekeris, Phys. Rev. **126**, 1470 (1962).
[40] Lijun Zhang (unpublished).